Long-range antiferromagnetic order in epitaxial Mn_2GaC thin films from neutron reflectometry

A. S. Ingason,[1,*] G. K. Pálsson,[2,3] M. Dahlqvist,[1] and J. Rosen[1]

[1]*Thin Film Physics, Department of Physics, Chemistry and Biology (IFM), Linköping University, SE-581 83 Linköping, Sweden*

[2]*Department of Physics and Astronomy, Uppsala University, Box 516, SE-75120 Uppsala, Sweden*

[3]*Institut Laue-Langevin, 38000 Grenoble, France*

(Received 3 March 2016; revised manuscript received 31 May 2016; published 13 July 2016)

The nature of the magnetic structure in magnetic so-called MAX phases is a topic of some controversy. Here we present unpolarized neutron-diffraction data between 3.4 and 290.0 K and momentum transfer between $Q = 0.0$ and 1.1 Å^{-1}, as well as complementary x-ray-diffraction data on epitaxial thin films of the MAX phase material Mn_2GaC. This inherently layered material exhibits neutron-diffraction peaks consistent with long-ranged antiferromagnetic order with a periodicity of two structural unit cells. The magnetic structure is present throughout the measured temperature range. The results are in agreement with first-principles calculations of antiferromagnetic structures for this material where the Mn-C-Mn atomic trilayers are found to be ferromagnetically coupled internally but spin flipped or rotated across the Ga layers. The present findings have significant bearing on the discussion regarding the nature of the magnetic structure in magnetic MAX phases.

DOI: 10.1103/PhysRevB.94.024416

Ever since Shull and Smart solved the antiferromagnetic structure of MnO in 1949—the efforts of which lead, in part, to the Nobel prize in physics in 1994—neutron diffraction has been an indispensable tool to examine magnetic order in condensed matter [1].

Neutron diffraction is often assumed not to be applicable to thin films due to the lack of sample volume [2], in spite of several successful such studies [3,4] already published. We will use and extend this method using an instrument designed for neutron reflectometry with a larger wavelength (5 Å) than in these previous studies, which maximizes the signal-to-background ratio at low momentum transfers.

The focus of the present paper is MAX phases, materials that naturally form laminated structures at the atomic level and exhibit a combination of metallic and ceramic properties [5]. The stoichiometry is of the type $M_{n+1}AX_n$, with $n = 1,2$, or 3 where M is an element of the early transition metals, A is an A-group element, and X is carbon or nitrogen. It has been suggested [6] that MAX phases could be of interest for applications within spintronics and calorimetry due to the peculiar laminated structure and potentially tuneable anisotropic transport properties.

Several papers have been published dealing with magnetism in MAX phases since they were first predicted [7], i.e., Cr_2AlC where A = Al, Ga, Ge, and systems with Mn partially substituting Cr on the M site. These include experimental work on bulk samples [8–13] and thin films [14–19] as well as further theoretical studies [14,19–24]. The magnetic behavior has been linked to itinerant-electron ferromagnetism, spin-density-wave states, Pauli paramagnetism, etc. This wide array of different magnetic behaviors is made more palpable by the different synthesis methods used and varying sample quality. In all these studies the Mn content and the local ordering between Mn and Cr may very likely have a critical impact on the magnetism observed. It is therefore of fundamental importance to establish the magnetic behavior thoroughly in those systems where chemical order plays no role, i.e., systems with only one M element as in the case of the Cr-based phases or the recently discovered Mn_2GaC, predicted by *ab initio* calculations and subsequently synthesized by thin-film techniques [25]. Such results could serve as a baseline for further studies of alloyed phases.

The magnetic behavior of MAX phases has been studied with first-principles density functional theory [7,22–24,26] where the identified magnetic ground states are generally different antiferromagnetic (AFM) structures with the ferromagnetic (FM) structure close in energy. For Mn_2GaC in particular, considered spin configurations include nonmagnetic, paramagnetic, FM, and multiple AFM configurations. Details regarding these calculations can be found in [27]. The identified low-energy magnetic ground-state candidates include the FM structure and two different AFM structures, labeled AFM$[0001]_2^A$ and AFM$[0001]_4^A$. The latter configuration is shown in Fig. 1(a) with four subsequent coparallel Mn layers followed by spin flip across an A layer. These structures have magnetic repetition distances of one (12.55 Å) and two (25.1 Å) unit cells, respectively. Performing neutron diffraction probing this length scale, well above the first allowed reflections from the structure, i.e., half the unit cell ($d = 6.275$ Å), is therefore needed in order to potentially demonstrate or falsify the existence of such ground-state candidates. In this paper we will show evidence for long-ranged antiferromagnetism of an epitaxially grown phase-pure single crystal of Mn_2GaC film of the highest quality [25].

Due to the spin of the neutron, even unpolarized neutron diffraction is sensitive to AFM order [28,29]. As an example, if there are spin configurations that exhibit periodicity, the neutrons will interfere constructively and peaks emerge in accordance with the magnetic structure factor. The nuclear structure factor captures the nonmagnetic contributions to the diffraction pattern and is given by

$$S_{\text{nuclear}} = \left| \sum_j b_j e^{-i\mathbf{Q}\mathbf{R}_j} \right|^2, \quad (1)$$

*arnsi@ifm.liu.se

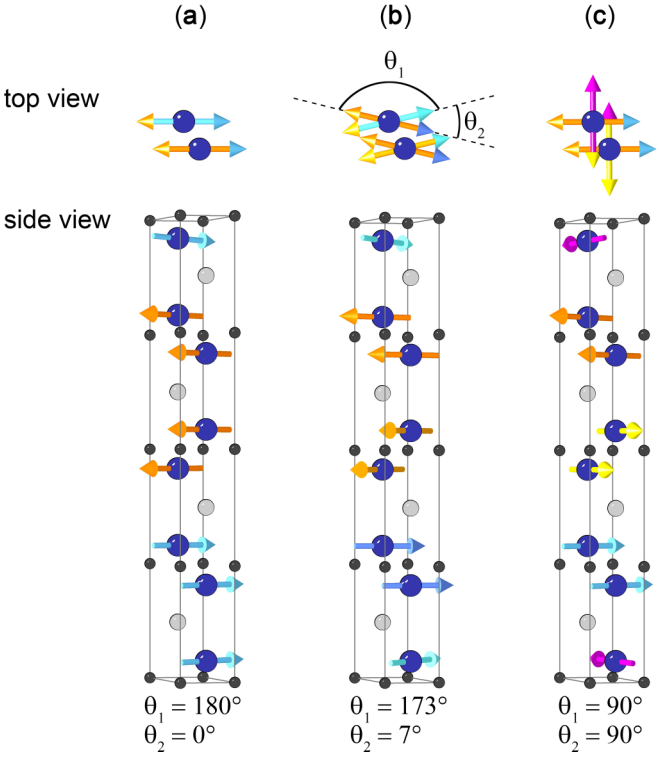

FIG. 1. Schematic of three antiferromagnetic spin configurations with alternating rotation of spins of Mn by θ_1 and θ_2 when passing the A layer. These represent low-energy structures found using first-principles calculations.

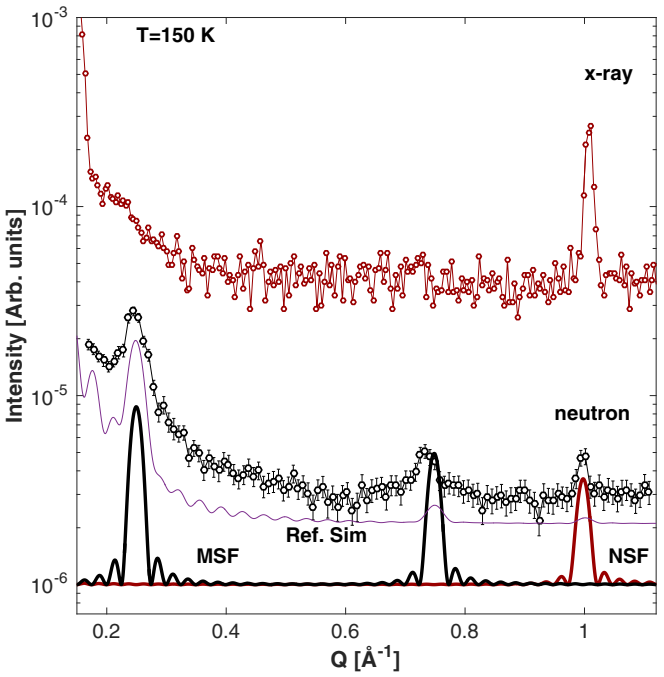

FIG. 2. X-ray-diffraction data of 50 nm of Mn_2GaC (top curve), unpolarized neutron diffraction (open black points), and reflectivity slab model of the AFM$[0001]_4^A$ structure (purple solid thin line). The magnetic structure factor (MSF) is shown as black solid lines for the same model and the nuclear structure factor (NSF) is shown as a solid red line.

where $\mathbf{Q}$ is the scattering vector with length $(4\pi/\lambda)\sin(\theta)$ where λ is the wavelength of the neutron and θ is the scattering angle, $\mathbf{R_j}$ is the coordinate of the jth atom, and b_j is the bound nuclear scattering length of element j. The simplified magnetic structure factor used in this study is similar but is sensitive to the spin arrangement as follows:

$$S_{\text{magnetic}} = \left| \sum_l f_l(\mathbf{Q}) \sigma_l e^{-i\mathbf{Q}\mathbf{R}_\mathbf{l}^\mathbf{s}} \right|^2, \qquad (2)$$

where σ_l is -1 for spin l aligned in the positive x direction and $+1$ for spin l aligned in the negative x direction, $\mathbf{R}_\mathbf{l}^\mathbf{s}$ is the position vector of the lth spin, and $f_l(\mathbf{Q})$ is the magnetic form factor.

The sample was grown using magnetron sputter epitaxy on 1×1-in. MgO (111) substrates at 823 K. The procedure followed the sample preparation and characterization found in [25] and was optimized according to [30]. The neutron measurements were performed at the Insitut-Laue-Langevin at the Super Adam reflectometer. This instrument is equipped with a highly oriented pyrolytic graphite monochromator with a wavelength of $\lambda = 5.183$ Å and a wavelength spread of 0.7%. The slits were 5 mm and as such the measurements were conducted with a high resolution of $\Delta Q_z = 5 \times 10^{-3}$ Å^{-1}. Thus the peak broadening is dominated by noninstrumental effects. The wavelength of 5.183 Å is above the cutoff for Bragg scattering from Al, which constituted the windows into the cryostat and the window into the evacuated flight path. We can thus eliminate any coherent Bragg scattering from Al and other materials such as Cu and Cd as well as the MgO substrate.

The scattering measurements were made with constant slits and the data were corrected for overillumination, incident flux changes, time, and direct beam intensity. The background was subtracted by taking the average of regions on either side of the specular peak. At every temperature the sample was realigned after confirming that thermal equilibrium had been reached.

Figure 2 shows unpolarized neutron diffraction at 150 K at remanence (2 mT, stray field from the electromagnet) (black line open circles) and x-ray diffraction (red line open circles) at the same temperature. The x-ray-diffraction pattern exhibits a single peak that appears at a position corresponding to the (0002) planes of the phase, i.e., $Q = 1.00$ Å^{-1}. No other structural peaks are visible below this peak in momentum transfer. In sharp contrast to the x-ray-diffraction data, three peaks can be identified in the neutron data at 0.25, 0.75, and 1.00 Å^{-1}. The peak at 1.00 Å^{-1} coincides with the x-ray data and we conclude that this peak is structural (nuclear scattering) in origin. Comparing to the previously suggested AFM$[0001]_4^A$ structure, a simple structure factor calculation using the coordinates for its atomic positions in Eq. (1) reveals that no structural peaks are expected below the (002) peak (red solid line). Inserting the coordinates for the on-site spins in the AFM$[0001]_4^A$ configuration into Eq. (2) reveals that an AFM structure of this type exhibits peaks at 0.25 and 0.75 (solid black line) but not at 1.00 Å^{-1}. The length scale corresponding to the 0.25 peak is ~25 Å or twice the structural unit cell. Furthermore, we can use the full width at half maximum of

the magnetic peaks to estimate the coherence length using $L = 2\pi/\Delta Q_{\mathrm{fwhm}} \approx 20$ nm. Thus we conclude that we have long-ranged antiferromagnetic order in Mn_2GaC that is very similar to the AFM$[0001]_4^A$ configuration.

The presented data are measured at small values of the momentum transfer Q and overlap with the neutron reflectivity region. The increase in the background signal at low Q is due to the Fresnel-type scattering. To demonstrate this effect and to further establish the validity of our results we divided the AFM$[0001]_4^A$ model into monolayers, each with its own magnetization direction and amplitude. The reflectivity program GenX [31] was used for the simulations, which takes into account total external reflection, refraction, and multiple reflections. We add up all the spin channels to mimic the unpolarized measurements and can see that the magnetic and the structural peaks are reproduced (purple thin line). We also see the rise in the signal at the lowest Q values. We note the absence of Kiessig (Laue) fringes in our data that probably is a result of surface roughness or thickness variation throughout the film. Those features are not directly relevant to the magnetic structure determination and no effort was made to reproduce them.

Figure 3 shows neutron diffraction at 3.4 K and 1 T applied field and at 150 and 290 K in a field of 2 mT. No significant changes are observed at the lowest temperature, which is expected since more than 5 T is required to saturate Mn_2GaC at this temperature, according to previous work [27]. At 290 K we see that an AFM structure is still present but the peaks

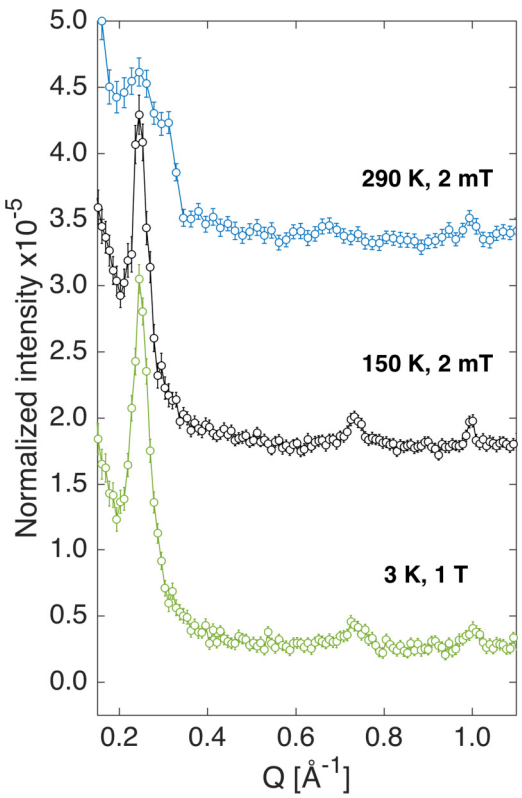

FIG. 3. Temperature dependence of the unpolarized neutron-diffraction data. The top curve is taken at 290 K, the middle curve is taken at 150 K, and the bottom curve is measured at 3.4 K. The applied field is around 2 mT except for the lowest temperature where the field was 1 T.

have split or broadened. This indicates an additional AFM structure with a slightly different repeat distance (propagation vector). Further work is needed to establish the Neel and Curie temperatures of this material.

It is highly desirable to obtain precise coordinates for all the atoms and an estimate of the magnitude of the magnetic moments. The procedure for this is to measure polarized neutron diffraction and x-ray diffraction in a wide Q range and apply an appropriate refinement technique. The present data are insufficient in this respect; however, they allow for far reaching qualitative conclusions as shown above. Given the uncertainty in the literature to date regarding the nature of magnetism in MAX phases, we claim that the present measurements provide the salient features of the magnetic structure, i.e., AFM order with a periodicity of two unit cells. Although the previously mentioned AFM$[0001]_4^A$ structure has this feature, so may other spin configurations. To identify such potential candidates, we performed *ab initio* calculations based on density functional theory using the projector augmented wave method [32] as implemented within VASP [33,34]. Exchange and correlation effects were treated in the framework of the Perdew-Burke-Ernzerhof [35] generalized gradient approximation in its spin-polarized form. We have used a plane-wave energy cutoff of 400 eV, and integration of the Brillouin zone was performed using the Monkhorst-Pack scheme [36]. The calculated total energy for all structures included in the present study is converged to within 0.1 meV/atom in terms of k-point sampling and plane-wave energy cutoff. Structural optimizations were performed for each spin structure in terms of unit-cell volumes, cell shape, and internal atomic positions to minimize the total energy.

The diversity of potential spin configurations considered is illustrated by the following identified low-energy structures, also shown in Fig. 1; (a) the collinear AFM$[0001]_4^{A,0/180}$, which is equivalent to AFM$[0001]_4^A$, with spins being rotated 180°, after every second Mn-C-Mn trilayer; (b) the noncollinear AFM$[0001]_2^{A,7/173}$, where each Mn-C-Mn trilayer is of alternating spin direction, being alternatively rotated in-plane by 7 and 173°, respectively, upon passing the Ga layer; and (c) AFM$[0001]_2^{A,90/90}$, where each trilayer is rotated 90°. The general notation of the noncollinear structures is then AFM$[0001]_2^{A,\theta_1/\theta_2}$. Corresponding energy differences for noncollinear configurations with respect to AFM$[0001]_4^{A,0/180}$ are +0.1 and +1.4 meV/atom, respectively. All three configurations are equivalent in terms of being consistent with the neutron reflectometry results shown in the present paper.

Previous reports on Mn_2GaC have shown a FM component in the hysteresis loop (vibrating sample magnetometry), indicating more complicated structures than the pure AFM. The structure (b) in Fig. 1 is consistent with the observed hysteresis loops and the results point towards this structure either being slightly favored in terms of energy over a symmetric structure, e.g., (a), or them being equal in energy. Once enough energy has been applied, the spin canting angle gradually changes more with applied field. The calculations show [see Fig. 6(b) in [27]] that there is almost no energy difference between the symmetric structure and any spin canting up to 7°. Hence, the remanence at zero field points towards degenerate ground states and to the fact that all these spin structures are populated

with the same statistical weight in the absence of applied field. Above 7° the energy increases gradually with canting angle but so does the energy of the applied field. Further measurements are needed to verify this claim, including magnetic measurements at a lower temperature and higher field.

We have established unambiguously that epitaxially grown Mn_2GaC on MgO [111] has an AFM structure with magnetic repetition distance of twice the structural unit cell (25 Å). The AFM$[0001]_4^A$ structure explains most features of the data but more data in a wider Q range and polarization analysis are needed to fully establish the complete magnetic order. The present results provide unambiguous evidence of long-range AFM order in MAX phase materials.

The research leading to these results has received funding from the European Research Council (ERC) under the European Community's Seventh Framework Programme FP7/2007-2013 (ERC Grant No. 258509). J.R. acknowledges funding from the Swedish Research Council Grant No. 621-2012-4425 and the Knut and Alice Wallenberg Foundation program. The Swedish Research Council is further acknowledged for support of the SuperADAM reflectometer at the Institut Laue-Langevin, Grenoble. The calculations were carried out using supercomputer resources provided by the Swedish national infrastructure for computing at the National Supercomputer Centre. Dr. Andrew Wildes is gratefully acknowledged for illuminating discussions.

[1] C. G. Shull and J. S. Smart, Phys. Rev. **76**, 1256 (1949).
[2] W. Kuch, L. I. Chelaru, F. Offi, J. Wang, M. Kotsugi, and J. Kirschner, Phys. Rev. Lett. **92**, 017201 (2004).
[3] H. Ott, C. Schüßler-Langeheine, E. Schierle, A. Yu. Grigoriev, V. Leiner, H. Zabel, G. Kaindl, and E. Weschke, Phys. Rev. B **74**, 094412 (2006).
[4] V. Leiner, K. Westerholt, B. Hjörvarsson, and H. Zabel, J. Phys. D **35**, 2377 (2002).
[5] M. W. Barsoum, M. W. Barsoum, and T. El-Raghy, Am. Sci. **89**, 334 (2001).
[6] J. Rosén, M. Dahlqvist, S. I. Simak, D. R. McKenzie, and M. M. M. Bilek, Appl. Phys. Lett. **97**, 073103 (2010).
[7] M. Dahlqvist, B. Alling, I. A. Abrikosov, and J. Rosén, Phys. Rev. B **84**, 220403 (2011).
[8] M. Jaouen, P. Chartier, T. Cabioch, V. Mauchamp, G. André, and M. Viret, J. Am. Ceram. Soc. **96**, 3872 (2013).
[9] Z. Liu, T. Waki, Y. Tabata, and H. Nakamura, Phys. Rev. B **89**, 054435 (2014).
[10] Z. Liu, T. Waki, Y. Tabata, K. Yuge, H. Nakamura, and I. Watanabe, Phys. Rev. B **88**, 134401 (2013).
[11] S. Lin, P. Tong, B. S. Wang, Y. N. Huang, W. J. Lu, D. F. Shao, B. C. Zhao, W. H. Song, and Y. P. Sun, J. Appl. Phys. **113**, 053502 (2013).
[12] Q. Z. Tao, C. F. Hu, S. Lin, H. B. Zhang, F. Z. Li, D. Qu, M. L. Wu, Y. P. Sun, Y. Sakka, and M. W. Barsoum, Mater. Res. Lett. **2**, 192 (2014).
[13] A. Mockute, J. Lu, E. J. Moon, M. Yan, B. Anasori, S. J. May, M. W. Barsoum, and J. Rosén, Mater. Res. Lett. **3**, 16 (2014).
[14] A. S. Ingason, A. Mockute, M. Dahlqvist, F. Magnus, S. Olafsson, U. B. Arnalds, B. Alling, I. A. Abrikosov, B. Hjörvarsson, P. O. Å. Persson, and J. Rosén, Phys. Rev. Lett. **110**, 195502 (2013).
[15] M. Jaouen, M. Bugnet, N. Jaouen, P. Ohresser, V. Mauchamp, T. Cabioc'h, and A. Rogalev, J. Phys.: Condens. Matter **26**, 176002 (2014).
[16] A. Petruhins, A. S. Ingason, J. Lu, F. Magnus, S. Olafsson, and J. Rosén, J. Mater. Sci. **50**, 4495 (2015).
[17] R. Salikhov, A. S. Semisalova, A. Petruhins, A. S. Ingason, J. Rosén, U. Wiedwald, and M. Farle, Mater. Res. Lett. **3**, 156 (2015).
[18] A. Mockute, P. O. Å. Persson, F. Magnus, A. S. Ingason, S. Olafsson, L. Hultman, and J. Rosén, Phys. Status Solidi RRL **8**, 420 (2014).
[19] A. Mockute, M. Dahlqvist, J. Emmerlich, L. Hultman, J. M. Schneider, P. O. Å. Persson, and J. Rosén, Phys. Rev. B **87**, 094113 (2013).
[20] M. Ramzan, S. Lebègue, and R. Ahuja, Phys. Status Solidi RRL **5**, 122 (2011).
[21] M. Ramzan, S. Lebègue, and R. Ahuja, Solid State Commun. **152**, 1147 (2012).
[22] M. Mattesini and M. Magnuson, J. Phys.: Condens. Matter **25**, 035601 (2013).
[23] M. Dahlqvist, B. Alling, and J. Rosén, J. Appl. Phys. **113**, 216103 (2013).
[24] M. Dahlqvist, B. Alling, and J. Rosen, J. Phys.: Condens. Matter **27**, 095601 (2015).
[25] A. S. Ingason, A. Petruhins, M. Dahlqvist, F. Magnus, F. Magnus, A. Mockute, B. Alling, L. Hultman, I. A. Abrikosov, P. O. Å. Persson, and J. Rosén, Mater. Res. Lett. **2**, 89 (2013).
[26] N. Li, C. C. Dharmawardhana, K. L. Yao, and W. Y. Ching, Solid State Commun. **174**, 43 (2013).
[27] M. Dahlqvist, A. S. Ingason, B. Alling, F. Magnus, A. Thore, A. Petruhins, A. Mockute, U. B. Arnalds, M. Sahlberg, B. Hjörvarsson, I. A. Abrikosov, and J. Rosén, Phys. Rev. B **93**, 014410 (2016).
[28] G. L. Squires, *Introduction to the Theory of Thermal Neutron Scattering*, 3rd ed. (Cambridge University, Cambridge, England, 2012).
[29] S. W. Lovesey and J. W. Lynn, Physics Today **39**, 64 (1986).
[30] A. S. Ingason, A. Petruhins, and J. Rosén, Mater. Res. Lett. (2016).
[31] M. Björck and G. Andersson, J. Appl. Cryst. **40**, 1174 (2007).
[32] P. E. Blöchl, Phys. Rev. B **50**, 17953 (1994).
[33] G. Kresse and J. Hafner, Phys. Rev. B **49**, 14251 (1994).
[34] G. Kresse and J. Hafner, Phys. Rev. B **48**, 13115 (1993).
[35] J. P. Perdew, K. Burke, and M. Ernzerhof, Phys. Rev. Lett. **77**, 3865 (1996).
[36] H. J. Monkhorst and J. D. Pack, Phys. Rev. B **13**, 5188 (1976).